Scheduling of Satellite Constellation Operations in EO Missions Using Quantum Optimization

(Article begins on next page)

Scheduling of Satellite Constellation Operations in EO Missions using Quantum Optimization

Vinicius Marchioli[1], Mattia Boggio[1], Deborah Volpe[1], Luca Massotti[2], and Carlo Novara[1]

[1] Politecnico di Torino, 10124 Turin, Italy
vinicius.marchioli@studenti.polito.it, mattia.boggio@polito.it, deborah.volpe@polito.it, carlo.novara@polito.it
[2] European Space Agency - ESTEC, Noordwijk, The Netherlands
luca.massotti@esa.int

Abstract. As Earth Observation (EO) missions advance towards Agile Earth Observation Satellites, the complexity of scheduling problems increases, posing challenges for traditional optimization methods. This paper investigates the potential of a quantum algorithm to address the scheduling problem in EO constellations. In particular, a novel formulation of the satellite constellation optimization problem is proposed, translating it into a Quadratic Unconstrained Binary Optimization (QUBO) problem, i.e., compliant with quantum solvers. Penalty functions are incorporated to optimize mission energy consumption. The formulated QUBO problem is then implemented and solved on a real quantum computer (a D-Wave Quantum Annealer). The performance provided by the quantum machine is compared with established classical meta-heuristic solvers like Simulated Annealing and Tabu Search. The results show that the proposed quantum optimization process achieves better results in terms of both solution quality and computational efficiency.

Keywords: Quantum optimization · QUBO · Earth Observation mission · Satellite Constellation Scheduling

1 Introduction

As space exploration becomes increasingly accessible through both private and governmental entities, Earth Observation (EO) missions have emerged as a critical area of concern and interest [4,35]. They aid scientific research, particularly in studying natural phenomena [9, 16, 28] and climate change dynamics [4, 14], and they may enhance national security by monitoring borders and resources [10]. Over the past decades, the EO missions have seen a significant transformation moving from long-lasting, multi-functional satellites, such as SPOT, ENVISAT, and ERS [11], to Agile Earth Observation Satellites (AEOSs). AEOSs are smaller and more agile satellites, where an extra degree of freedom around the pitch axis enables the satellites for fast and precise orientation changes in nadir. They operate in Low Earth Orbits (LEO), often in constellations, and can perform specific

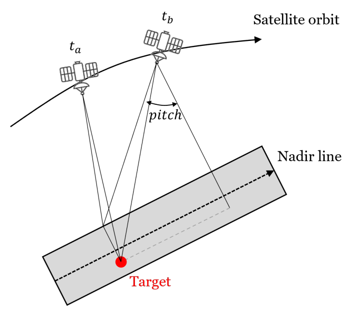

(a) AEOS's enhanced manoeuvrability around the pitch axis.

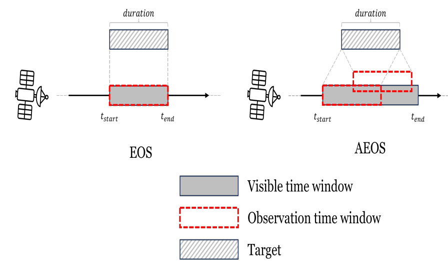

(b) Comparison of the observation capability of EOS and AEOS.

Fig. 1: Agile Earth Observation Satellites (AEOSs).

tasks efficiently [30, 32]. Fig. 1a shows the additional manoeuvrability of these satellites, while in Fig. 1b the main difference in observation capability between Non-Agile Earth Observation Satellite (EOS) and AEOS is illustrated. For the EOS, the specific Observation Time Window (OTW), which is the time period required for the satellite to observe a specific area on Earth, coincides with its Visible Time Window (VTW), namely the time period when the target is physically visible to the satellite's instruments. In contrast, AEOSs have expanded observation capabilities, offering multiple feasible OTWs for a single target.

While the agile characteristic greatly improves the observation efficiency and flexibility of AEOS, it also significantly increases the complexity of the scheduling problem for EO missions. This problem consists of selecting and scheduling satellite observation tasks to maximize the entire observation profit while satisfying all the operational constraints. For traditional EOS, the scheduling problem is relatively straightforward as VTW coincides with OTW. Instead, for AEOS, each VTW contains multiple potential OTWs, resulting in a considerable expansion in the search space for scheduling observations. This makes the scheduling problem NP-hard and thus potentially challenging for traditional optimization methods. Indeed, these approaches may either struggle to find a global solution or require too long execution times to achieve satisfactory results. The limitations of traditional approaches become even more pronounced when dealing with constellations of AEOS, namely the case study considered in this paper, where the complexity of the scheduling problem increases further.

With the rise of quantum technologies, it is becoming clear that quantum computers have the potential to significantly improve the efficiency and quality of solutions to complex optimization problems [3, 27]. There are two different approaches for leveraging quantum computers in the optimization context: gate-based quantum computing [5] and adiabatic quantum computation (AQC) [2]. In the gate model, the computation is performed by applying a series of unitary gates to a set of quantum bits (qubits), which can be measured at the end of the computation, for developing various algorithms including optimization ones. On the other hand, in AQC, an initial multi-qubit quantum state is prepared as the ground state of a simple Hamiltonian, followed by an adiabatic time evolution that transforms the system into a final Hamiltonian whose ground state represents the solution of an optimization problem. This paper focuses on AQC and in particular on the Quantum Annealing (QA) paradigm, which exploits the adiabatic principle to solve optimization problems [22]. The first company to develop a real quantum annealer was D-Wave in 2011 [17].

Recent literature has provided substantial demonstrations of the applicability of quantum computers and algorithms to address real-world optimization challenges. For instance, in [23], a D-Wave quantum annealer is used for peptide and protein design tasks. Furthermore, a novel approach that uses the quantum annealing paradigm and D-Wave's machines for optimizing traffic light control in urban areas was introduced in [21]. Other application domains in which quantum computing has already been exploited include, e.g., machine learning [6], cryptography [26], finance [24], and logistics [33].

In the realm of aerospace applications, a pioneering work that applies the quantum paradigm to the scheduling problem of EO missions is [29]. This work investigates the potential and maturity of then-available quantum computers for solving a "small-scale" scheduling problem, using a Quadratic Unconstrained Binary Optimization (QUBO) formulation. A comparative analysis is conducted between traditional optimization methodologies and a D-Wave 2000Q quantum annealer. The results show that the quantum annealer can be faster and its solution quality is comparable for "small" problems, but it degrades for larger ones due to the limited qubit connectivity and noise issues.

Following the line of [29], the present paper explores the use of a Dwave quantum annealer, using in particular a Hybrid quantum annealing algorithm (HQA) [8], for an EO constellation scheduling problem, comparing its performance to established classical meta-heuristic solvers like Simulated Annealing (SA) [19] and Tabu Search (TS) [13]. The HQA is a hybrid classical/quantum algorithm that implements state-of-the-art classical algorithms with intelligent allocation of the Dwave Quantum Processing Unit (QPU) to suitable parts of the problem in order to speed up the execution and enhance solutions for large problem sizes. In summary, the main contributions of our study are the following: (i) Formulation of the satellite constellation optimization problem and translation into a QUBO problem. To the best of our knowledge, this is the first work that provides a rigorous and complete formulation of this problem for a constellation of several satellites. (ii) Integration of penalty functions in the optimization problem, allowing us to reduce the propellant consumption of the mission, i.e. extending the lifetime. (iii) Implementation and solution of the obtained QUBO problem on a real quantum annealer. Note that the implementation is not trivial since the choice of the annealer setting and related parameters may be quite complex and/or critical. Moreover, we solve QUBO problems with a significantly larger number of decision variables than the existing works considering similar mission planning problems. (iv) Extensive simulations, using a real D-Wave quantum annealer, and comparison with state-of-the-art QUBO solvers running on classical computers.

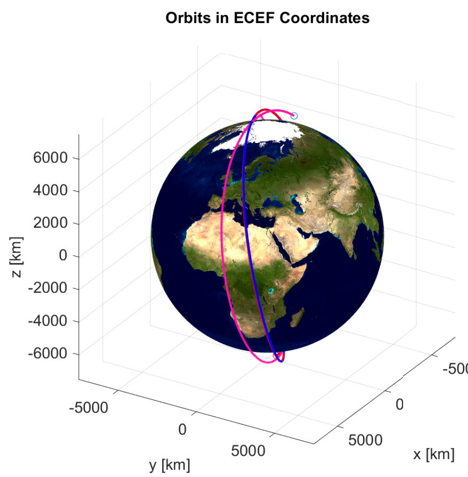

(a) Constellation orbits over the globe.

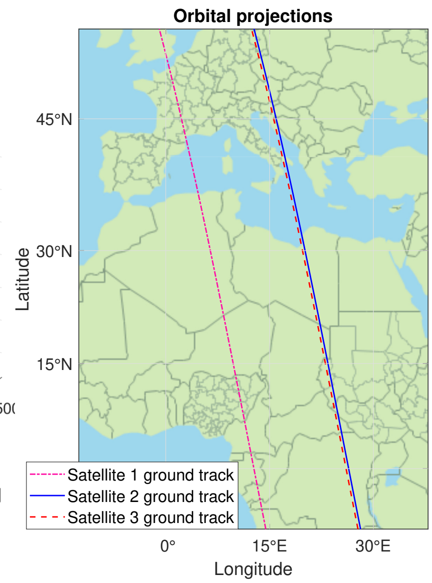

(b) Orbital projections over Europe and Africa.

Fig. 2: Example of a three-satellite constellation, characterized by heliosynchronous, highly polar, circular orbits.

This article is organized as follows. Section 2 introduces the mathematical formulation of the constellation scheduling problem. Section 3 presents the translation of this formulation into a QUBO problem. In section 4, the mission scenario for the EO scheduling problem is described and a comparative analysis of the results obtained using the quantum annealer and classical solvers is presented. Finally, the conclusions are drawn in Section 5.

2 Constellation Scheduling Problem

Consider a constellation of N_S satellites traveling on different orbits. The three-satellite constellation, considered in this study and characterized by heliosynchronous, highly polar, circular orbits, is depicted in Figs. 2a and 2b. In particular, Fig. 2a depicts the S/C orbits over the globe, while Fig. 2b shows the orbital projections over Europe and Africa. It should be noted that the QUBO formulation developed in this paper is general and does not depend on the particular constellation considered. Here, we have chosen to use the SuperView-1 constellation, which consists of Chinese commercial and remote sensing satellites [31]. Although Satellites 2 and 3 share similar orbits, they can be used to observe different targets, thereby reducing fuel consumption. For more details, please refer to Section 4.

The orbits are designed in such a way that an arc of each orbit lies above a given region of the Earth containing N_T targets. When a satellite is traveling in its orbit, it spends a fraction of the orbit period on the arc above the region and, in this time interval, it can acquire observations/images of the targets. The fraction of the orbit period spent on the arc is called Visible Time Window (VTW). The orbit arc is divided into smaller segments, corresponding to sub-intervals of duration ΔT of the VTW. While flying on a segment, a satellite can acquire observations of a subset of targets. For simplicity, a single orbital revolution is considered, so that a target may be observed by a satellite no more than once. The goal is to find an optimal observation scheduling for the satellites of the constellation. To formalize the optimization problem, the following quantities are defined:

- $S \doteq \{1, \ldots, N_S\}$: Satellite index set. An index $j \in S$ indicates the jth satellite of the constellation.
- $T \doteq \{1, \ldots, N_T\}$: Target index set. An index $i \in T$ indicates the ith target.
- VTW_{ji}, $i \in T$, $j \in S$: Orbit segment index set. VTW_{ji} contains the indices associated to the orbit segments from which the jth satellite can acquire an image of the ith target. The indices in VTW_{ji} are ordered by increasing traveling time.
- $w_{jik} \in \mathbb{R}_{\geq 0}$, $j \in S$, $i \in T$, $k \in VTW_{ji}$: Profit associated to a target. w_{jik} is related to the priority of acquiring an image of the ith target. The priority may depend on the satellite and the orbit segment.
- $\xi_{jik} \in \{0, 1\}$, $j \in S$, $i \in T$, $k \in VTW_{ji}$: Decision variable. ξ_{jik} indicates if the jth satellite has acquired an image of the ith target while flying in the orbit segment with index $k \in VTW_{ji}$. $\xi_{jik} = 1$ if the acquisition has been accomplished, $\xi_{jik} = 0$ otherwise.
- $n = \sum_{j=1}^{N_S} \sum_{i=1}^{N_T} \mathrm{card}(VTW_{ji})$: Number of decision variables $\xi_{jik} \in \{0, 1\}$. Note that, in general, $n \leq N_S N_T$.
- $\zeta \doteq (\xi_{j_1 i_1 k_1}, \ldots, \xi_{j_n i_n k_n}) \in \{0, 1\}^n \subset \mathbb{N}^{n \times 1}$, $j_1, \ldots, j_n, \in S$, $i_1, \ldots, i_n \in T$, $k_1 \in VTW_{j_1 i_1}, \ldots\ k_n \in VTW_{j_n i_n}$: Vector containing all the decision variables. The order in which the ξ_{jik}'s appear in ζ is arbitrary. The one adopted in this paper is as follows: $ijk \in \{111, 112, \ldots,\ 121, 122, \ldots,\ 211, 212, \ldots,$ $221, 222, \ldots\}$. The symbol $\mathbb{N}$ denotes the set of natural numbers including 0.

Based on these definitions, the ideal profit of the whole mission is

$$J_P \doteq \sum_{i \in T} \sum_{j \in S} \sum_{k \in VTW_{ji}} w_{jik} \xi_{jik} \,.$$

In this work, we have chosen to make a single acquisition for each target in order to avoid excessive fuel consumption. This can be imposed by the following constraints:

$$\sum_{j \in S} \sum_{k \in VTW_{ji}} \xi_{jik} \leq 1, \ \forall i \in T \,. \tag{1}$$

It must also be taken into account that the observation of two consecutive targets may be not feasible, since there may be not enough time for a satellite to maneuver from one acquisition to the subsequent one. The following constraints avoid to plan unfeasible consecutive observations:

$$\begin{aligned}\xi_{ji_1k_1} + \xi_{ji_2k_2} \leq 1,\ &\forall j \in S\,,\\ &\forall i_1, i_2 \in T, i_1 \neq i_2, \forall (k_1,k_2) \in F_{ji_1i_2}\,,\end{aligned} \tag{2}$$

where $F_{ji_1i_2}$ is a so-called forbidden maneuver region. This set is defined as

$$\begin{aligned}F_{ji_1i_2} \doteq \{&(k_1,k_2) \in VTW_{ji_1} \times VTW_{ji_2} :\\ &\tau_{ji_2k_2} < \tau_{ji_1k_1} + T_F\}\,,\end{aligned}$$

where τ_{jik} is the start time of the ith target acquisition, accomplished by the jth satellite from the kth orbit segment, and T_F is the sum of the duration of an acquisition and the duration of the maneuver.

In order to penalize acquisitions which require a high attitude adjustment and thus a high fuel consumption, the following term is introduced:

$$J_C \doteq \sum_{i \in T} \sum_{j \in S} \sum_{k \in VTW_{ji}} \lambda_{jik} \xi_{jik}\,.$$

Finally, we define the objective function

$$J(\zeta) \doteq -J_P + J_C,$$

where $\zeta \doteq (\xi_{111}, \xi_{112}, \ldots, \xi_{121}, \ldots, \xi_{211}, \ldots, \xi_{N_S 11}, \ldots)$.

To sum up, an optimal observation scheduling for the satellites of the constellation can be found by solving the following optimization problem:

$$\begin{aligned}\zeta^* = \arg &\min_{\zeta \in \{0,1\}^n} J(\zeta)\\ &\text{subject to :}\\ &(i)\ \sum_{j \in S} \sum_{k \in VTW_{ji}} \xi_{jik} \leq 1,\ \forall i \in T\\ &(ii)\ \xi_{ji_1k_1} + \xi_{ji_2k_2} \leq 1,\ \forall j \in S\,,\\ &\qquad \forall i_1, i_2 \in T, i_1 \neq i_2, \forall (k_1,k_2) \in F_{ji_1i_2}\,.\end{aligned} \tag{3}$$

In general, (3) is an Integer Linear Programming (ILP). Due to the discrete nature of the decision variables, this kind of problem is NP-hard for a classical computer. Quantum computers and, in particular, quantum annealers have the potential to significantly reduce the computational complexity of these classes of problems, finding better solutions with a polynomial speedup compared to classical computers [3]. A formulation of the optimization problem (3) that is compliant with quantum annealers is called QUBO (Quadratic Unconstrained Binary Optimization) and is developed in the next section.

3 QUBO Formulation

In this section, the optimization problem of Equation (3) is formulated according to the QUBO model [12]. In the QUBO formulation, the objective function is of the form

$$H = \zeta^\top \mathbf{Q}\, \zeta\,, \tag{4}$$

where $\mathbf{Q} \in \mathbb{R}^{n\times n}$ is a matrix of real numbers and $\zeta \in \{0,1\}^n \subset \mathbb{N}^{n\times 1}$ is a vector of binary variables. This optimization model can consider a constraint only through an aggregation method. In particular, it is taken into account by including in the function a quadratic penalty function, assuming a value of 0 for configurations satisfying the constraints and a positive amount otherwise.

The operations needed to obtain the QUBO formulation (4) of the optimization problem (3) are now described in detail.

The function $J(\zeta)$ can be written as

$$\begin{aligned} J &\doteq -J_P + J_C \\ &= \sum_{i\in T}\sum_{j\in S}\sum_{k\in VTW_{ji}} (\lambda_{jik} - w_{jik})\xi_{jik} \\ &= \sum_{i\in T}\sum_{j\in S}\sum_{k\in VTW_{ji}} (\lambda_{jik} - w_{jik})\xi_{jik}^2\,, \end{aligned}$$

where it has been considered $\xi_{jik} = \xi_{jik}^2$, $\forall j, i, k$.

The constraints (1) are translated into the following penalty terms:

$$\rho_i \doteq \frac{1}{2}\sum_{j_1,k_1,j_2,k_2} \xi_{j_1ik_1}\xi_{j_2ik_2}\,,\ \forall i \in T\,,$$

for all $j_1, j_2 \in S$, $k_1 \in VTW_{j_1i}$, $k_2 \in VTW_{j_2i}$, $(j_2,k_2) \neq (j_1,k_1)$. It can be easy verified that $\rho_i = 0$ if and only if the constraint $\sum_{j\in S}\sum_{k\in VTW_{ji}} \xi_{jik} \leq 1$ is satisfied.

In a similar way, the constraints (2) are translated into the following penalty terms:

$$\begin{aligned} \eta_l \doteq \xi_{ji_1k_1}\xi_{ji_2k_2}\,,\ &\forall j \in S\,, \\ &\forall i_1, i_2 \in T, i_1 \neq i_2, \forall (k_1,k_2) \in F_{ji_1i_2}\,, \end{aligned}$$

where $l = 1,\ldots,N_U$ and N_U is the number of unfeasible maneuvers. Also the penalties η_l are in the QUBO compatible format, i.e. expressed as a quadratic penalty function, and give nonzero off-diagonal elements in the $\mathbf{Q}$ matrix.

The following objective function can now be defined:

$$H \doteq -J_P + J_C + \Lambda\left(\sum_{i=1}^{N_T}\rho_i + \sum_{l=1}^{N_U}\eta_l\right)\,, \tag{5}$$

where Λ is a positive real number. If Λ is properly sized, the minimizers of H are solutions of the optimization problem (3). However, its dimensioning is not trivial since its value has to be sufficiently high to penalize invalid solutions without flattening the problem function too much, avoiding effective solution space explorations.

While J_P represents the ideal profit of the mission, $-H$ gives the profit adjusted by the penalties. The quantity $-H$ is thus called Practical Profit.

A fundamental observation is that H is a quadratic function of $\zeta = (\zeta_1, \ldots, \zeta_n) \doteq (\xi_{j_1 i_1 k_1}, \ldots, \xi_{j_n i_n k_n})$, so it is compliant with the QUBO formulation (4). The construction of the matrix $\mathbf{Q}$ is simple and can be accomplished considering that the coefficients $\lambda_{jik} - w_{jik}$ of $J = -J_P + J_C$ are on the main diagonal of $\mathbf{Q}$, whereas the penalty terms ρ_i and η_l give off-diagonal entries equal to Λ. In detail, let $q_{\alpha\beta}$, $\alpha, \beta = 1, \ldots, n$ be the entries of $\mathbf{Q}$. Then, $\mathbf{Q}$ is constructed as follows:

- $\text{diag}(\mathbf{Q}) = (p_{j_1 i_1 k_1}, \ldots, p_{j_n i_n k_n})$, $p_{jik} \doteq \lambda_{jik} - w_{jik}$.
- $q_{\alpha\beta} = \Lambda$ if, for some i, the term $\zeta_\alpha \zeta_\beta$ is contained in ρ_i, or, for some l, it is contained in η_l.
- $q_{\alpha\beta} = 0$ otherwise.

Once $\mathbf{Q}$ has been defined according to these indications, a typical operation is to make $\mathbf{Q}$ symmetric by posing $\mathbf{Q} := (\mathbf{Q} + \mathbf{Q}^T)/2$. This operation does not change the optimization problem and allows us to use QUBO solvers that require symmetric matrices $\mathbf{Q}$.

The objective function (5) is thus equal to $H = \zeta^\top \mathbf{Q}\, \zeta$, and the resulting optimization is written in the QUBO form

$$\zeta^* = \arg \min_{\zeta \in \{0,1\}^n} \zeta^\top \mathbf{Q}\, \zeta. \tag{6}$$

For sufficiently large values of Λ, the solutions of (6) are also solutions of the optimization problem (3). Similarly to (3), also the optimization problem (6) is NP-hard for a classical computer. As discussed above, quantum annealers may overcome the limitations of classical solvers in this context.

3.1 Quantum annealers

Quantum annealers [17, 18] are special-purpose quantum computers suitable to solve QUBO problems like (6) with a significant computational speedup (quadratic) compared to classical computers [7, 34], possibly improving also the solution quality. Now, we summarize what is a quantum annealer and how it works. Defining

$$\sigma = (\sigma_1, \ldots, \sigma_n) \doteq 2\zeta - I \in \{-1, 1\}^n \subset \mathbb{Z}^{n \times 1},$$

the QUBO objective can be written as

$$H = \zeta^\top \mathbf{Q}\, \zeta = \frac{1}{4}(\sigma + I)^\top \mathbf{Q}\, (\sigma + I) = \frac{1}{4}\sigma^\top \mathbf{Q}\sigma + \frac{1}{2} I^\top \mathbf{Q}\sigma + \frac{1}{4} = H_F + \frac{1}{4}.$$

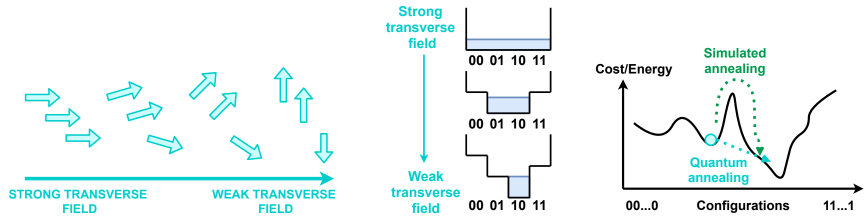

(a) Spins evolution during annealing. When a strong transverse field is applied, spins are in a superposition state. Reducing the transverse field, spins assume a spin-down or spin-up state to reach the lowest energy configuration.

(b) Quantum annealer system evolution explained through a simple *hydraulic model*.

(c) Quantum tunneling *vs.* thermal climbing. The first represents the exploration mechanism of quantum annealing, while the second that of simulated annealing.

Fig. 3: Overview of quantum annealing.

The function H_F defined as

$$H_F \doteq \sigma^\top J_F \sigma + h_F \sigma, \quad J_F \doteq \frac{1}{4}\sigma^\top \mathbf{Q}, \quad h_F \doteq \frac{1}{2} I^\top \mathbf{Q} \tag{7}$$

is called transverse-field Ising Hamiltonian and represents the energy of a physical system consisting of n interacting particles, described by two-state variables σ_i, $i = 1, \ldots, n$ (e.g., spin of electrons, polarization of photons, superconducting loops, etc.). A Quantum Annealer (QA) is indeed a lattice of n interacting nodes, called qubits, described by two-state variables, which obey the laws of quantum mechanics. They are physically implemented by means of superconducting loops [15, 17]. While a bit of a classical computer is allowed to be in one of two possible states, a qubit can be in a superposition of both states simultaneously. This property, peculiar of quantum systems, enables the so-called quantum parallelism, where the computer can explore simultaneously multiple solutions of a problem, unlike classical computers that explore only one solution at a time. Such a parallelism is one of the key features of QAs. Another important feature is quantum tunneling, which allows the computer to bypass energy barriers, thus reducing the issue of trapping in local solutions, as shown in Fig. 3c. The main steps accomplished by a QA to solve a QUBO-like problem are as follows.

Quantum Annealing Process

1. *Initialization:* The QA system is initialized in a superposition of states, representing all the possible configurations of the optimization problem. It means that each qubit is in a superposition of its basis state 0 and 1. The corresponding initial Hamiltonian is denoted by H_I. This can be graphically represented by the spins aligned on the x-axis of Fig. 3a or by the flat bottom of the tank in the hydraulic model usually exploited for explaining QA system evolution of Fig. 3b.

2. *Adiabatic evolution:* The Hamiltonian is continuously modified from H_I, whose ground state is easily configured as initial state, to the final Hamiltonian H_F in (7), which encodes the optimization problem. The evolution is controlled in an adiabatic manner, in such a way that the QA remains in the ground state during the whole process, also avoiding local minima thanks to quantum tunneling. The evolution is described by $H_{QA} = \varphi(t)H_I + (1 - \varphi(t))H_F$, where H_{QA} is the QA Hamiltonian and $\varphi(t)$ is a continuous function of time such that $\varphi(0) = 1$ and $\varphi(T_A) = 0$, being $T_A > 0$ called the annealing time. This can be graphically represented in Fig. 3b with the hydraulic model as a gradual deformation of the tank's bottom for describing the objective function, and the water begins to flow towards the lowest points. Alternatively, it can be represented as spins of 3a which start to modify their orientation to assume the lowest energy configuration.
3. *Measurement:* Once the evolution process is complete, the final spin vector σ^* is measured. This vector corresponds to a minimum of the Hamiltonian which, at the end of the process, is $H_F = H - 1/4$. It follows that the solution of the QUBO problem (6) is $\zeta^* = (\sigma^* + I)/2$.
4. *Post-processing:* The obtained solution might not be perfect due to noise and defects in the quantum hardware. Post-processing techniques like classical optimization algorithms can be used to refine the solution (e.g., simulated annealing or tabu search).
5. *Repetitions:* The whole procedure (steps 1 - 4) can be repeated several times and the best result is selected. □

After the initialization step, the system is a superposition condition, guaranteeing a simultaneous and parallel exploration of the solution space, giving an exponential speedup with respect to a classical computer, where the solutions must be explored one at a time. However, the evolution from the initial to the final Hamiltonian cannot be arbitrarily fast. The Adiabatic Theorem states that a quantum system starting from a ground state persists in a ground state, provided that the change in time of the Hamiltonian is sufficiently slow. Let T_A be the annealing time, i.e., the time taken to change the Hamiltonian from H_I to H_F. According to the Adiabatic Theorem, the ground state is maintained during the change if

$$T_A \geq \frac{1}{\min_{t \in [0, T_A]} \Delta E(t)^2} , \tag{8}$$

where ΔE is the gap between the two lowest energy levels of the QA. The combination of the exponential speedup in the initialization step and the limit imposed by the Adiabatic Theorem yield in any case a significant computational complexity reduction with respect to classical computers. Indeed, despite it is notoriously difficult to analyze the runtime of adiabatic optimization algorithms, several works in the literature show that a quadratic speedup with respect to classical computers can be guaranteed [7, 34].

If inequality (8) is not satisfied, there is a non-null probability for the QA to jump from the lowest energy level to the second lowest level, or even to higher

Table 1: OE for the satellite constellation.

ID	a (km)	i (°)	Ω (°)	e	ω (°)	ν (°)
1000	6903.67	97.58	97.85	16.55e−4	130.99	2.03
2000	6909.06	97.58	93.20	9.97e−4	254.46	155.23
3000	6898.60	97.58	92.36	14.60e−10	276.73	140.19

energy levels, which correspond to sub-optimal solutions of the optimization problem. This gives rise to a trade-off between computational speed and quality of the solution: sub-optimal solutions can be found, which require a shorter annealing time with respect to an optimal solution but are satisfactory in practice.

A leading company in the field of QAs is D-Wave Systems [1], which is developing QAs with a growing number of qubits (more than 5000), enabling the solution of increasingly complex optimization problems. Quantum annealing is still an evolving technology, and there are ongoing efforts worldwide to improve its performance and reliability.

4 Simulation Results

In this section, the proposed quantum algorithm is validated and compared with the following classical meta-heuristic algorithms: Tabu Search (TS) [13] and Simulated Annealing (SA) [19]. Firstly, the mission scenario for the EO scheduling problem is described in detail. Then, a comprehensive analysis of the results obtained considering both quantum and classical algorithms is reported.

4.1 Mission scenario description

The scenario considered in this paper for the EO scheduling problem is shown in Fig. 4a. It includes a list of all the European capitals and many UNESCO Natural World Heritage sites. The main characteristics of the scenario are shown below:

1. Number of decision variables: 1471.
2. Number of unique targets: 55.
3. Constraint density: 22.51%.

To accomplish this mission, three satellites have been taken into account. Their parameters, presented in Table 1, are based on the well-documented SuperView-1 constellation consisting of Chinese commercial and remote sensing satellites [31], launched in 2018. Their agile nature allows to perform maneuvers in the roll and pitch directions, with a range of ±45°, for both angles.

The first column shows the unique ID of the S/Cs, while the OE are presented from columns 2 to 7, respectively: semi-major axis a, inclination i, right ascension of the ascending node Ω, eccentricity e, argument of perigee ω and mean anomaly ν. From the original specifications, the orbital elements (OE) for satellite 1, with ID 1000, is slightly modified to fit the generated data requirements for sparsity.

These OE account for heliosynchronous, highly polar and almost circular orbits. One orbital revolution for the constellation is around 95 minutes.

The chosen profit, from 1 to 5, and duration are arbitrarily selected to be as generic as possible while still preserving the realistic nature of the problem. Alongside the ground tracks, two auxiliary roll lines, computed during the pre-treatment phase, are plotted, providing a good visual indication of each satellite's line-of-sight reach (as can be seen in Fig. 4a). In practice, the down-sampled data are used for the problem formulation, considerably reducing the number of variables, but still maintaining the system's physical characteristics and real-world applicability [31]. Some authors prefer a finer resolution [25], while others [20] opt for an even larger time step. It should be noted that this scenario consists of a high-density dataset due to the close vicinity and the number of targets. Indeed, satellites two and three may observe more than 30 targets in less than 10 minutes with many overlapping VTWs. Consequently, the resulting $\mathbf{Q}$ matrix is highly dense, making the problem hard to solve, especially with QA, as it requires more physical qubits to embed the variable relations.

4.2 Results comparison

The tests conducted in this study involved the implementation of the proposed strategies using Matlab for QUBO formulation. Then, depending on the strategy used, these QUBO problems were solved using different solvers provided by D-Wave. In particular: i) the `D-Wave Leap Hybrid Sampler` for the HQA, ii) the `D-Wave SimulatedAnnealingSampler` for the SA, and iii) the `D-Wave TabuSampler` for the TS.

Note that, before deciding to use the HQA, we carefully compared it with pure QA, finding that nowadays the latter is not able to produce satisfactory solutions for large-scale problems. This is due to the known problems of quantum hardware, such as environmental noise, a limited number of physical qubits, and intricate problem-embedding strategies.

To evaluate the performance, the algorithms under consideration were executed 100 times in order to obtain a comparative distribution. The metrics used for the comparison are: i) the mean value of the Practical Profit $-H$ (Mean Pract. Profit $-H$), ii) its standard deviation (SD Pract. Profit $-H$), iii) the mean value of the Runtime (Mean Runtime), and iii) its standard deviation (SD Runtime).

Taking into account the characteristics of the scenario described in Section 4.1, it can be observed that, although the targets across Europe are densely geographically distributed, the resulting matrix exhibits only around 22% constraint density. Nevertheless, as the number of decision variables increases, the complexity of solving the problem escalates considerably. Indeed, classical solvers experience a decline in performance, highlighting the efficacy of adopting the hybrid quantum approach. Considering the best outcome of the 100 executions of the HQA, a maximum Practical Profit of 103.33 was obtained with 40 unique targets captured. This result is visually depicted in Fig. 4b.

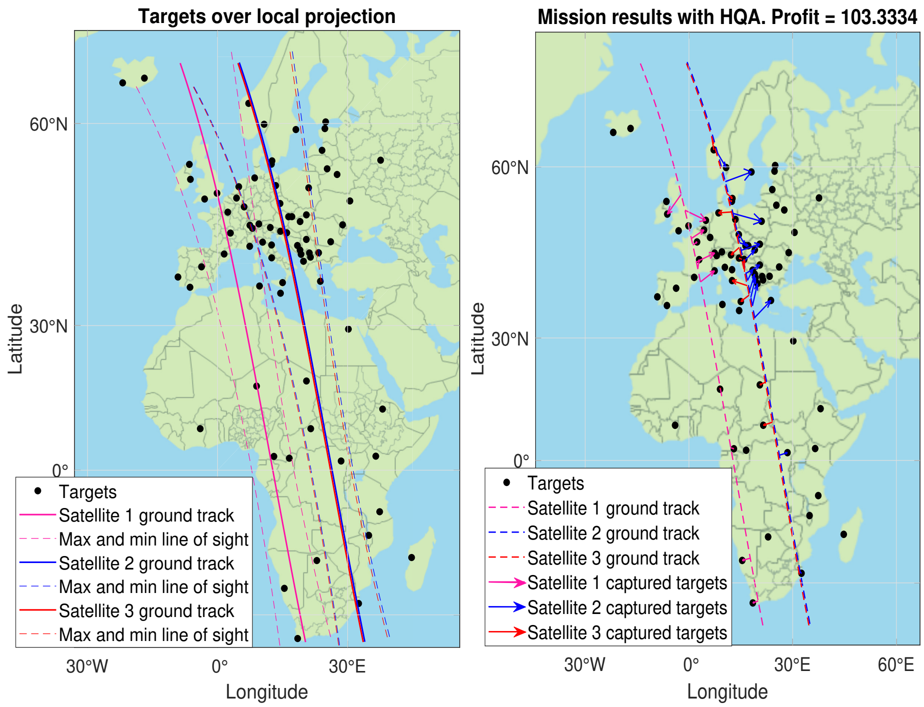

(a) Target disposition and constellation ground tracks over local projection.

(b) Captured targets over Europe and Africa with HQA.

Fig. 4: EO scheduling problem.

Table 2 collects the mean results of all the 100 executions of the three algorithms, based on the metrics previously described. All the methods yield viable and feasible mission results with comparable Practical Profit $-H$ and, most importantly, without any constraint violation. However a clear advantage of the HQA can be noted in terms of runtime. On average, it is 1.6 times faster than TS and 6 times faster than SA. Additionally, from the outcomes of the 100 mission, a comparative distribution is presented in Fig. 5. The HQA outperforms its classical counterparts not only in terms of mean values but also by yielding a lower standard deviation, with more reliable results. These remarkable results were obtained using around 40 ms of QPU access time with respect to the 4 s of total runtime, showing the effectiveness of combining the classical metaheuristics with quantum methods. It should be noted that, ideally, increasing the number of reads can improve the quality of optimal solutions obtained with

Table 2: Comparison between classic and hybrid quantum algorithms.

	Mean Pract. Profit $-H$	SD Pract. Profit $-H$	Mean Runtime (s)	SD Runtime (s)
TS	90.76	1.07	6.96	1.31
SA	99.23	0.74	25.46	2.83
HQA	101.94	0.37	4.0140	0.0038

classical solvers. However, this approach may not be feasible for real-time satellite scheduling due to the time constraints involved. Additionally, it leads to an increase in the standard deviation of the associated profit, negatively impacting overall solution precision.

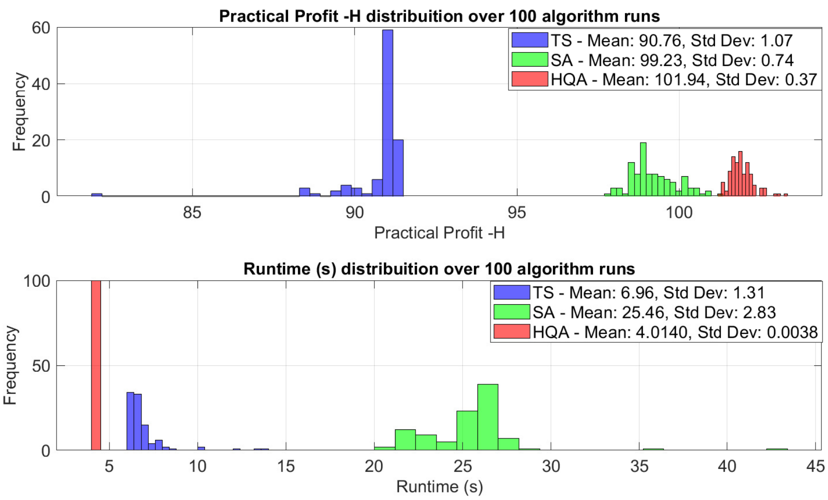

Fig. 5: Results distribution for 100 runs.

5 Conclusions

In conclusion, this paper introduces a novel QUBO formulation for the AEOSs scheduling problem. This formulation has been implemented onto the real Dwave quantum computer using the HQA approach and compared with classical optimization solvers, such as SA and TS. The obtained results show improved performance in terms of both quality of the solutions and computational time, suggesting that hybrid techniques are ready to be used in real and scalable mission scenarios

The proposed formulation could be further improved by relaxing model constraints for broader applicability and introducing an integer-valued unicity constraint that allows multiple target acquisitions. Additionally, despite the increased in complexity, the solver could potentially handle a one-day scheduling horizon, effectively simulating real missions. Finally, a reconfigurable model for movable targets could optimize both orbital adjustments and target acquisition. It is important to note that the current quantum devices are limited in terms of number of qubits availability, connectivity and fidelity. These limitations necessitate the use of hybrid solvers for contemporary industrial applications. Despite these challenges, the results obtained are encouraging. They demonstrate that exploring quantum solutions can provide valuable insights for the future of real-time satellite scheduling research.

Acknowledgement. We would like to thank D-Wave Systems for providing access to their quantum annealer through the free monthly user program.

References

1. D-wave systems. https://www.dwavesys.com/
2. Albash, T., Lidar, D.A.: Adiabatic quantum computation. Rev. Mod. Phys. **90**, 015002 (Jan 2018)
3. Albash, T., Lidar, D.A.: Demonstration of a scaling advantage for a quantum annealer over simulated annealing. Physical Review X **8**(3), 031016 (2018)
4. Anderson, K., Ryan, B., Sonntag, W., Kavvada, A., Friedl, L.: Earth observation in service of the 2030 agenda for sustainable development. Geo-spatial Information Science **20**(2), 77–96 (2017)
5. Barenco, A., Bennett, C.H., Cleve, R., DiVincenzo, D.P., Margolus, N., Shor, P., Sleator, T., Smolin, J.A., Weinfurter, H.: Elementary gates for quantum computation. Phys. Rev. A **52**, 3457–3467 (Nov 1995)
6. Biamonte, J., Wittek, P., Pancotti, N., Rebentrost, P., Wiebe, N., Lloyd, S.: Quantum machine learning. Nature **549**(7671), 195–202 (2017)
7. Boixo, S., Ortiz, G., Somma, R.: Fast quantum methods for optimization. The European Physical Journal Special Topics **224**(1), 35–49 (2015)
8. Booth, M., Reinhardt, S.P., Roy, A.: Partitioning optimization problems for hybrid classical/quantum execution. Technical Report pp. 01–09 (2017)
9. Chuvieco, E., Mouillot, F., van der Werf, G.R., San Miguel, J., Tanase, M., Koutsias, N., García, M., Yebra, M., Padilla, M., Gitas, I., Heil, A., Hawbaker, T.J., Giglio, L.: Historical background and current developments for mapping burned area from satellite earth observation. Remote Sensing of Environment **225**, 45–64 (2019)
10. Dolce, F., Di Domizio, D., Bruckert, D., Rodríguez, A., Patrono, A.: Earth Observation for Security and Defense, pp. 705–731. Springer International Publishing (2020)
11. Dubock, P.A., Spoto, F., Simpson, J., Spencer, D., Schutte, E., Sontag, H.: The Envisat satellite and its integration. ESA Bulletin **106**, 26–45 (Jun 2001)
12. Glover, F., Kochenberger, G., Du, Y.: Quantum Bridge Analytics I: a tutorial on formulating and using QUBO models. 4OR **17**(4), 335–371 (12 2019)
13. Glover, F., Laguna, M.: Tabu search. Springer (1998)
14. Guo, H.D., Zhang, L., Zhu, L.W.: Earth observation big data for climate change research. Advances in Climate Change Research **6**(2), 108–117 (2015), special issue on advances in Future Earth research
15. Hauke, P., Katzgraber, H.G., Lechner, W., Nishimori, H., Oliver, W.D.: Perspectives of quantum annealing: Methods and implementations. Reports on Progress in Physics **83**(5), 054401 (2020)
16. Hirschmugl, M., Gallaun, H., Dees, M., Datta, P., Deutscher, J., Koutsias, N., Schardt, M.: Methods for mapping forest disturbance and degradation from optical earth observation data: A review. Current Forestry Reports **3**, 32–45 (2017)
17. Johnson, M.W., Amin, M.H., Gildert, S., Lanting, T., Hamze, F., Dickson, N., Harris, R., Berkley, A.J., Johansson, J., Bunyk, P., et al.: Quantum annealing with manufactured spins. Nature **473**(7346), 194–198 (2011)
18. Kadowaki, T., Nishimori, H.: Quantum annealing in the transverse ising model. Physical Review E **58**(5), 5355 (1998)
19. Kirkpatrick, S., Gelatt, C.D., Vecchi, M.P.: Optimization by simulated annealing. Science **220**(4598), 671–680 (1983)
20. Liu, X., Laporte, G., Chen, Y., He, R.: An adaptive large neighborhood search metaheuristic for agile satellite scheduling with time-dependent transition time. Computers & Operations Research **86**, 41–53 (2017)

21. Marchesin, A., Montrucchio, B., Graziano, M., Boella, A., Mondo, G.: Improving urban traffic mobility via a versatile quantum annealing model. IEEE Transactions on Quantum Engineering **4**, 1–13 (2023)
22. Morita, S., Nishimori, H.: Mathematical foundation of quantum annealing. Journal of Mathematical Physics **49**(12), 125210 (12 2008)
23. Mulligan, V.K., Melo, H., Merritt, H.I., Slocum, S., Weitzner, B.D., Watkins, A.M., Renfrew, P.D., Pelissier, C., Arora, P.S., Bonneau, R.: Designing peptides on a quantum computer. bioRxiv (2020)
24. Orús, R., Mugel, S., Lizaso, E.: Quantum computing for finance: Overview and prospects. Reviews in Physics **4**, 100028 (2019)
25. Peng, G., Song, G., Xing, L., Gunawan, A., Vansteenwegen, P.: An exact algorithm for agile earth observation satellite scheduling with time-dependent profits. Computers & Operations Research **120**, 104946 (03 2020)
26. Pirandola, S., Andersen, U.L., Banchi, L., Berta, M., Bunandar, D., Colbeck, R., Englund, D., Gehring, T., Lupo, C., Ottaviani, C., Pereira, J.L., Razavi, M., Shaari, J.S., Tomamichel, M., Usenko, V.C., Vallone, G., Villoresi, P., Wallden, P.: Advances in quantum cryptography. Adv. Opt. Photon. **12**(4), 1012–1236 (Dec 2020)
27. Roland, J., Cerf, N.J.: Quantum search by local adiabatic evolution. Physical Review A **65**(4) (Mar 2002)
28. Ruf, C., Unwin, M., Dickinson, J., Rose, R., Rose, D., Vincent, M., Lyons, A.: Cygnss: Enabling the future of hurricane prediction [remote sensing satellites]. IEEE Geoscience and Remote Sensing Magazine **1**(2), 52–67 (2013)
29. Stollenwerk, T., Michaud, V., Lobe, E., Picard, M., Basermann, A., Botter, T.: Agile earth observation satellite scheduling with a quantum annealer. IEEE Transactions on Aerospace and Electronic Systems **57**(5), 3520–3528 (2021)
30. Verfaillie, G., Lemaître, M.: Selecting and scheduling observations for agile satellites: Some lessons from the constraint reasoning community point of view. In: Principles and Practice of Constraint Programming - CP. pp. 670–684 (11 2001)
31. Wang, X., Han, C., Zhang, R., Gu, Y.: Scheduling multiple agile earth observation satellites for oversubscribed targets using complex networks theory. IEEE Access **7**, 110605–110615 (2019)
32. Wang, X., Wu, G., Xing, L., Pedrycz, W.: Agile earth observation satellite scheduling over 20 years: Formulations, methods, and future directions. IEEE Systems Journal **15**(3), 3881–3892 (09 2021)
33. Yarkoni, S., Huck, A., Schülldorf, H., Speitkamp, B., Tabrizi, M.S., Leib, M., Bäck, T., Neukart, F.: Solving the shipment rerouting problem with quantum optimization techniques. In: Mes, M., Lalla-Ruiz, E., Voß, S. (eds.) Computational Logistics. pp. 502–517. Springer International Publishing, Cham (2021)
34. Zanca, T., Santoro, G.E.: Quantum annealing speedup over simulated annealing on random ising chains. Phys. Rev. B **93**, 224431 (Jun 2016)
35. Zhao, Q., Yu, L., Du, Z., Peng, D., Hao, P., Zhang, Y., Gong, P.: An overview of the applications of earth observation satellite data: Impacts and future trends. Remote Sensing **14**(8) (2022)